nature chemistry

REVIEW ARTICLE

PUBLISHED ONLINE: 19 MARCH 2009 | DOI: 10.1038/NCHEM.121

Towards the computational design of solid catalysts

J. K. Nørskov[1]*, T. Bligaard[1], J. Rossmeisl[1] and C. H. Christensen[2]

Over the past decade the theoretical description of surface reactions has undergone a radical development. Advances in density functional theory mean it is now possible to describe catalytic reactions at surfaces with the detail and accuracy required for computational results to compare favourably with experiments. Theoretical methods can be used to describe surface chemical reactions in detail and to understand variations in catalytic activity from one catalyst to another. Here, we review the first steps towards using computational methods to design new catalysts. Examples include screening for catalysts with increased activity and catalysts with improved selectivity. We discuss how, in the future, such methods may be used to engineer the electronic structure of the active surface by changing its composition and structure.

During the past century chemists have developed efficient chemical reactions for converting fossil resources into a broad range of fuels and chemicals, and this can be considered one of the most important and far-reaching scientific developments up to now. Today, essentially all transportation fuels are refined in a number of catalytic processes and most chemicals are also produced using technologies based on catalysis[1]. A few well-known examples illustrate the impact: about half of all petrol in the world is now produced by fluid catalytic cracking using specially designed zeolite catalysts, and the Haber–Bosch process — featuring an iron catalyst — continues to have a key role in the production of fertilizers. The list of important small- and large-scale processes by which fossil resources are converted into fuels and chemicals is almost endless.

Such catalytic technologies have also resulted in various environmental issues — even the best processes do not allow a complete elimination of undesirable byproducts. Many innovative, catalytic technologies have subsequently been implemented to remedy these new problems; one famous example is the precious-metal-based three-way catalyst installed in most petrol-fuelled passenger cars. Moreover, these developments have contributed to an increased use of fossil resources and thus to the increasing carbon dioxide levels in the atmosphere. Currently, there is a significant drive to relinquish our dependence on fossil fuels and to minimize the emission of carbon dioxide. Clearly, this calls for many new and improved catalytic processes, and for catalytic technologies that focus on prevention rather than on remediation.

Reducing environmental impact will require entirely new catalysts: catalysts for new processes, more active and more selective catalysts and preferably catalysts that are made from earth-abundant elements. This represents a formidable challenge and it will demand an ability to design new catalytic materials well beyond our present capabilities. The ultimate goal is to have enough knowledge of the factors determining catalytic activity to be able to tailor catalysts atom-by-atom. The catalytic properties of a material are in principle determined completely by its electronic structure, so the objective is the engineering of electronic structure by changing composition and physical structure. The approach is illustrated in Fig. 1. Over the past few decades our understanding of why particular materials are good catalysts for given reactions has improved. The challenge is to invert this problem; given that we need to catalyse a certain reaction under a set of specified conditions, which material should we choose?

The aim of controlling matter at the molecular scale by engineering the electronic structure is not restricted to catalytic materials; it is a general challenge in chemistry, physics and materials science, and there is considerable progress in several areas such as materials for batteries[2], hydrogen storage[3], optical absorption[4] and molecules for homogeneous catalysis[5,6]. Catalysis at surfaces is particularly well suited for electronic structure engineering, primarily because the link between the atomic-scale properties and the macroscopic functionality — the kinetics — is well developed. In addition, the theoretical description of surface reactions has been enhanced considerably by the availability of a large number of quantitative experimental surface-science studies of adsorption and reaction phenomena[7–12].

Here, we review some of the first examples of the computer-based design of solid catalysts. We introduce a number of concepts linking catalytic performance to the properties of the catalyst's surface, and in turn discuss how the surface electronic structure determines the catalytic properties. Finally, we discuss some of the challenges ahead.

Trends and descriptors of catalytic activity

The extraordinary progress in density functional theory (DFT) calculations for surface processes is the key development that has created the possibility of computer-based catalyst design[13]. Current methods are fast enough to allow the treatment of complex, extended systems[14,15]. They can also now provide the interaction energies of molecules and atoms with metal surfaces with sufficient accuracy to describe trends in reactivity for transition metals and alloys[16].

There are now several cases where the complete kinetics of a catalytic reaction has been evaluated solely on the basis of DFT calculations of reaction barriers, reaction energies and the associated entropies[17–20]. Figure 2 shows the comparison between calculated and measured rates for three different reactions and catalytic surfaces. Overall, the agreement between DFT-based kinetic models and experiment is surprisingly good, and they serve to illustrate the accuracy and value of current density functional theory.

The agreement between theory and experiment is particularly noteworthy in two cases for supported metal catalysts (ruthenium

[1]Center for Atomic-scale Materials Design, Department of Physics, Building 311, Technical University of Denmark, DK-2800 Kgs. Lyngby, Denmark
[2]Haldor Topsøe A/S, Nymøllevej 55, DK-2800 Kgs. Lyngby, Denmark; *e-mail: norskov@fysik.dtu.dk

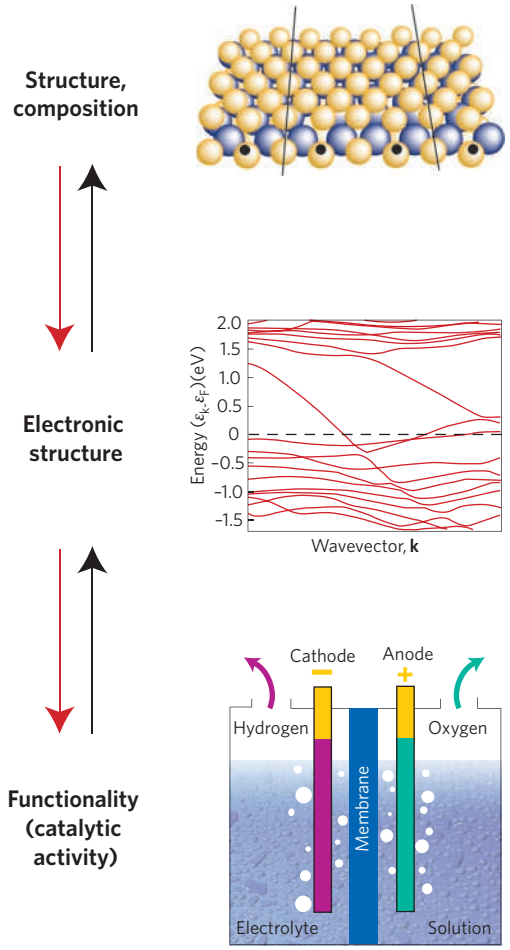

Figure 1 | Tailoring materials. Illustration of the way the electronic structure is the link between the structure and composition of a material and its functionality. Changing the functionality can be achieved by engineering the electronic structure through modification of structure and composition. The example shown is a MoS_2 sheet, a few atoms wide, where new electronic states at the edges cross the Fermi level and give rise to catalytic activity, for instance in electrochemical hydrogen evolution[63].

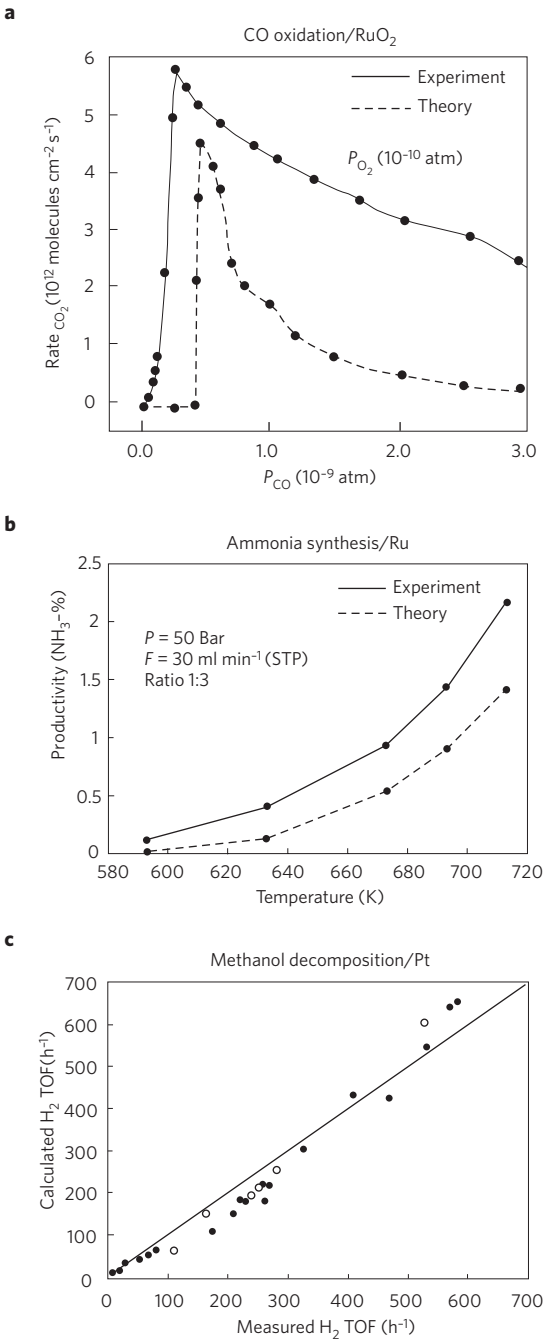

Figure 2 | Comparison of experimental results for three different catalytic reactions with the results of kinetic models based on DFT calculations. **a**, CO oxidation activity over ruthenium oxide at low oxygen pressures. Adapted from ref. 18; © 2004 APS. **b**, Ammonia synthesis productivity over a ruthenium catalyst at industrial reaction conditions. Based on data from ref. 19. **c**, Methanol decomposition rate over a platinum catalyst. In each of these three cases the theoretical calculations and the experiments agree semi-quantitatively. Adapted from ref. 20; © 2006 Springer.

and platinum in Fig. 2) — which are considerably more complex than a well-defined single crystal surface. Here, the theoretical treatment has assumed that the supported metallic nanoparticles can be viewed as crystalline particles with well-defined facets in addition to edges, corners, steps and kinks, and that these surface features can be treated as being independent of each other. Each surface structure will then contribute to the overall rate and the most active one will typically dominate. This is, for instance, the case for ammonia synthesis where step sites dominate[19]. Several experiments have shown real catalyst particles to have well-defined geometrical features[21–25]. The independence of the different types of surface sites on metal particles can be understood by noting that the electrostatic screening by the metallic, freely moving electrons introduces a 'nearsightedness'[26,27] such that a perturbation to the surface is only significant within a screening length — typically a few ångströms. For very small particles, where the electrons are no longer metallic, this picture breaks down — the exact size where this happens is still an open question.

The complete kinetic description of a given system is a quite demanding task. One cannot, at this moment, imagine screening a large number of systems using a procedure that requires such a description for each system considered. Rather, it is instructive to establish which properties at the atomic scale determine the macroscopic kinetics. Such an approach in terms of descriptors is outlined below.

The identification of descriptors is facilitated substantially by the observation that activation energies for elementary surface reactions are strongly correlated with adsorption energies. This is illustrated in Fig. 3 for the methanation reaction ($CO + 3H_2 \rightarrow CH_4 + H_2O$). First, it is established computationally that the activation barrier for CO dissociation is forbiddingly high on the most close-packed surface, whereas certain steps (and other similar geometries) have much lower barriers (by approximately 1 eV)[28,29]. The active site on

the catalyst surface is therefore identified as the steps or edges on the surface of the catalyst material.

On comparing a series of different metal surfaces as catalysts for the methanation reaction (Fig. 3a) it is found that the barrier for CO activation, as well as the barriers for CH_4 and H_2O formation, are closely related to the stability of C and O on the surface. The more stable they are, the lower the barrier for CO dissociation will be, and the higher the barrier becomes for CH_4 and H_2O formation. In fact, all three activation energies are found to scale essentially linearly with the reaction energy in Brønsted–Evans–Polanyi (BEP)-type relationships (see Fig. 3b for CO dissociation)[28,30–32]. Such correlations lead directly to a volcano relationship between the rate and the dissociative chemisorption energy, E_{diss}, of CO (ref. 33; see Fig. 3c). The reason is that in the limit of weak coupling (E_{diss} is only a little negative), the BEP relation gives that the barrier for dissociation of the reactants will be high and the rate low. For strong coupling (E_{diss} very negative) the activation energy of adsorption is small but now the barrier for forming the products will be large. An optimal interaction strength must exist between these two limits — this is known as the Sabatier principle[34]. Figure 3 shows that calculations can be used to quantify the interaction strength in such a way that experimental data for the methanation rates can be understood on this basis. E_{diss} is therefore a good descriptor for the catalytic activity of different catalysts for the methanation reaction, and we can identify its optimum value from Fig. 3.

In general there may be several descriptors, depending on the number of different important surface intermediates. The number of independent variables is limited strongly by the fact that it has been found that adsorption energies for a number of molecules scale with each other[35]. For the methanation reaction, for instance, the bond energy of adsorbed CH, CH_2 and CH_3 vary linearly with the bond energy of adsorbed C from one metal surface to the next, and the same is true for OH versus O adsorption energies.

Volcano relations between rates and adsorption energies have been widely identified in heterogeneous catalysis. For many years adsorption energies of intermediates were not readily available and various thermodynamic data, such as heats of oxide formation, were used as descriptors[36]. With the advent of sufficiently accurate DFT calculations this situation has completely changed, and descriptors of catalytic activity in terms of calculated adsorption energies have been identified for a number of systems[33,37,38].

The volcano-shaped relationships between total catalytic rates and adsorption energies may explain some of the good agreement between experiments and theory shown in Fig. 2. Close to the top of the volcano the rate depends only weakly on the absolute strength of the adsorption energies. For the methanation reaction, for instance, the window of values of E_{diss} around the maximum where the rate is within an order of magnitude of the maximum values is on the order of 0.5 eV. This means that for the best catalysts (close to the maximum of the volcano) errors of a few tenths of an eV may still give reasonable values for the rate. As this is the typical error of DFT calculations[15], they can give quite accurate rates at least close to the top of the volcano.

The electronic structure factor

The variation in adsorption energy (and hence the catalytic activity) from one metal to the next is determined by the electronic structure of the surface. It turns out that for the transition metals the coupling between the adsorbate valence states and the metal *d*-states largely describe the variations[39–44]. The rule is that the higher in energy the *d*-states are relative to the highest occupied state — the Fermi energy — of the metal, the stronger the interaction with adsorbate states. The reason is that when the *d*-states are close to the Fermi energy, antibonding states can be shifted well above it and become empty (or bonding states can be shifted below it and become occupied). This increases the bond strength. Figure 4a establishes how variations in adsorption energy from one metal to the next are correlated with shifts in the energy of the *d*-states. Figure 4b,c shows a more subtle effect: The electronic structure of a platinum surface can be engineered by inserting another metal (nickel, cobalt, iron and so on) in the second layer and this directly affects the oxygen and hydrogen adsorption energies. It shows how changing the metal ligands of the surface platinum atoms can change its chemical properties substantially.

Catalyst design

The first examples of where ideas generated from electronic structure calculations were exploited in the search for new solid catalysts include: the modification of the stability of Ni catalysts for steam reforming by the addition of gold[45]; the mixing of cobalt and molybdenum in ammonia synthesis catalysts[46]; new mixed transition metal sulfides for hydro-desulfurization[47]; new CO-tolerant alloys for fuel-cell anodes[48]; and near-surface alloys for hydrogen activation[49].

The first example of extensive computational screening of surface structures for new catalysts was for the methanation reaction[50]; this reaction is used extensively in industry to remove trace amounts of CO from hydrogen streams produced by steam-reforming of hydrocarbons[51].

The approach taken was as follows. First the CO dissociation energy, E_{diss}, was identified as a descriptor of catalytic activity as described above, and indicated in Fig. 3. The optimal value was identified by comparison to experimental data for the elemental metals, see Fig. 3c. Then a series of binary alloys (with concentration varying in steps of 25%) were formed from metals (Ni, Pd, Pt, Co, Rh, Ir, Fe, Ru and Re) chosen so that they should be reasonably stable

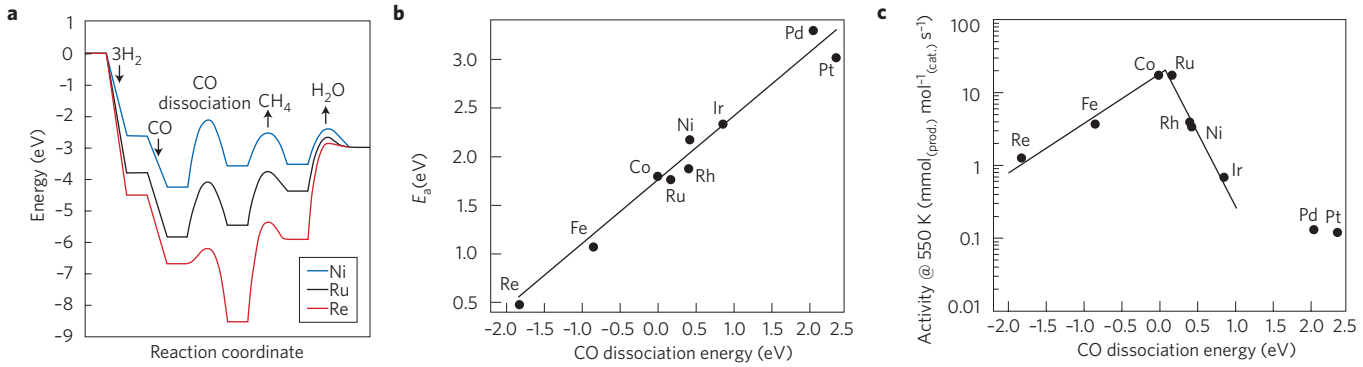

Figure 3 | Identification of a descriptor for the methanation reaction ($CO + 3H_2 \rightarrow CH_4 + H_2O$). a, Calculated energy diagrams for CO methanation over nickel, ruthenium and rhenium. Only the highest of the activation barriers for hydrogenation of C and O are included. **b**, Brønsted–Evans–Polanyi relation for CO dissociation over transition metal surfaces. The transition state potential energy, E_a, is linearly related to the CO dissociation energy. **c**, The corresponding measured volcano-relation for the methanation rate[33]. Parts **b** and **c** reprinted from ref. 50; © 2006 Elsevier.

at methanation conditions. For each alloy the catalytic performance descriptor $|E_{diss} - E_{diss}(optimal)|$ was then calculated using a simplified interpolation model. A total of 117 different systems were studied.

In the case of the methanation reaction, there are already elemental metals, ruthenium and cobalt, close to the top of the volcano, see Fig. 3c. These metals are, however, not used industrially because they are quite costly. Instead the cheaper but also inferior catalyst material Ni is used. The cost of the raw materials is therefore an important parameter, and in Fig. 5a all the alloys and elemental metals included in the study are shown in a cost versus catalytic performance plot. NiFe alloys stand out in this plot as having a high catalytic activity as well as a low price. They were therefore chosen for a more detailed theoretical and experimental study. This involved a full DFT calculation of the energetics to make sure that the simple interpolation model was correct. It also involved a series of computational tests of stability of the alloy towards segregation. The result of the experimental test is included in Fig. 5b. A series of catalysts supported on MgAl spinel were prepared and their methanation activities were measured. It can be seen that the NiFe alloys are indeed more active than both pure nickel and iron, as predicted. Subsequently, the concept was converted into a technical catalyst at Haldor Topsøe[52].

An example from electrocatalysis

Electro-catalysis design is currently attracting much attention mainly for energy-conversion purposes. Many future energy transformation processes rely on electro-catalysis. One important example is the evolution of hydrogen in electrolysis and the reverse process where hydrogen is used as a fuel in a fuel cell. In acidic solutions platinum is the preferred catalyst material for both processes. As a hydrogen electrode it is stable and effective, but it is scarce and expensive, and extensive research efforts are directed towards replacing it — or at least reducing the amount needed.

Compared with catalysts for gas-phase reactions, the description of electro-catalysts has additional challenges due to the liquid phase in direct contact with the catalysts surface and due to charging of the surface[53–58]. Another very important constraint is the corrosive environment that the catalyst is often exposed to in the electrolyte. Many of the non-precious catalyst materials important in conventional heterogeneous catalysis, for example, iron, cobalt or nickel, will quickly dissolve in acids.

The hydrogen-evolution reaction, where protons and electrons recombine to form molecular H_2, is one of the simplest electrochemical reactions, but still no good alternative to the platinum catalyst has been found. The adsorption free-energy of hydrogen, ΔG_{H^*}, is a good descriptor for hydrogen evolution[59–61]. This makes sense because no matter what the reaction path is, adsorbed hydrogen is one of the intermediates. If H binds too weakly to the surface, H^+ cannot adsorb from the dissolved phase and if it binds too strongly, it will have difficulty leaving the surface for the gas phase. One would expect the optimal rate when hydrogen at the surface is as stable as gas-phase hydrogen — which by definition has the same free energy as solvated protons and electrons at zero potential relative to the normal hydrogen electrode (see Fig. 6a). Plotting the exchange current density versus the binding of hydrogen obtained by DFT indeed shows a volcano with an optimum around zero free energy of adsorption[62] (see Fig. 6b).

A computational search for high activity can then be carried out by calculating ΔG_{H^*}. As stability of the catalyst is a major issue, the calculation of descriptors for stability is as important as for activity. A range of surface alloys (alloys only in the first layer) with the optimal combined stability and activity can then be indentified[63,64] (see Fig. 6c). One interesting candidate is a surface alloy of platinum and bismuth. Supported on pure platinum, adsorbed bismuth is known to poison hydrogen evolution[65], however, when the surface is annealed, a PtBi surface alloy is formed showing a measured activity slightly higher than that of a reference sample of pure platinum[64].

Another strategy for identifying materials that could have promising features as hydrogen-evolution catalysts is by taking inspiration from biology. Hydrogenases[66] and nitrogenases[67] are known to be good catalysts for hydrogen evolution. The descriptor approach also applies to the active centres of enzymes[63,68] (see

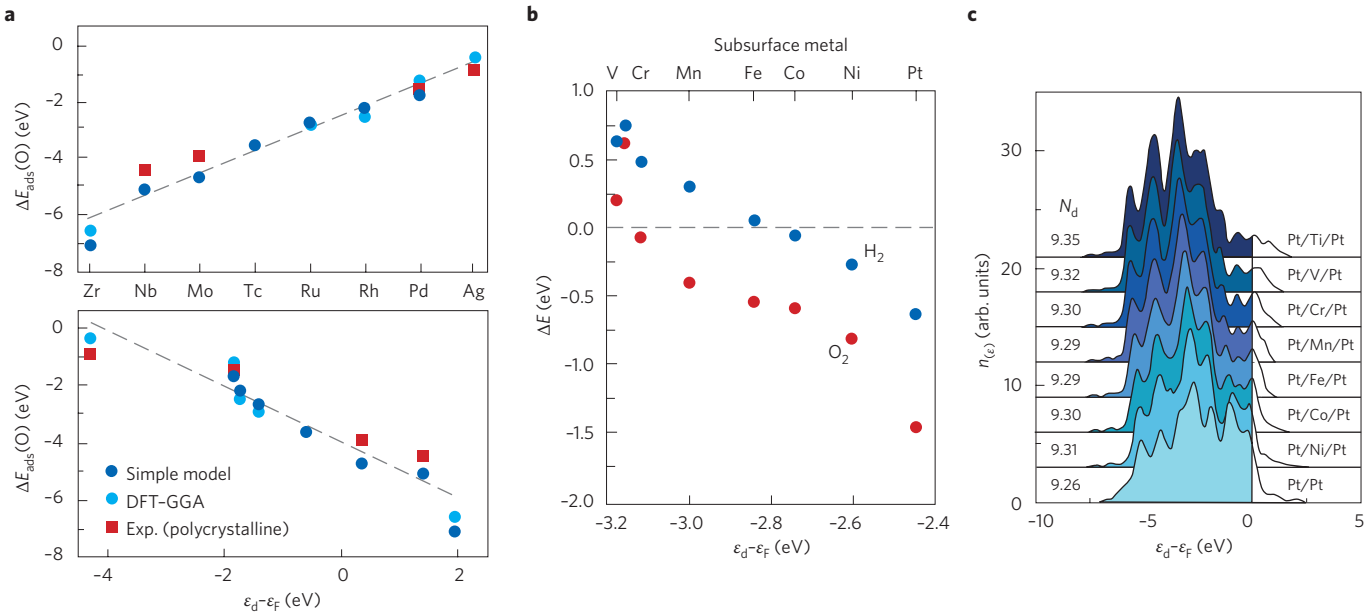

Figure 4 | The *d*-band model — understanding the electronic origin of variations in surface chemistry. a, Variations in the O adsorption energy, ΔE_{ads}(O), on the most close-packed surface of the 4*d* transition metal series. The results of full DFT calculations are compared with those from a simple Newns–Anderson model[98] and to experiments (polycrystalline surfaces)[9]. Below, the same data are plotted as a function of the average energy of the *d*-electrons (the *d*-band centre with respect to the Fermi level), ε_d-ε_F, on the transition metal. Adapted from ref. 16; © 2000 Elsevier. **b**, Calculated changes in the dissociative adsorption energy of H_2 and O_2, ΔE, versus the average energy of the projected density of states for the surface platinum *d*-states. **c**, Local projected densities of states, $n(\varepsilon)$, for a series of Pt(111) surfaces, where the second layer has been replaced by a layer of a 3*d* transition metals are shown. N_d is the number of *d* electron on the surface Pt atoms, which is hardly affected by the subsurface atoms. Parts **b** and **c** adapted from ref. 99; © 2004 Elsevier.

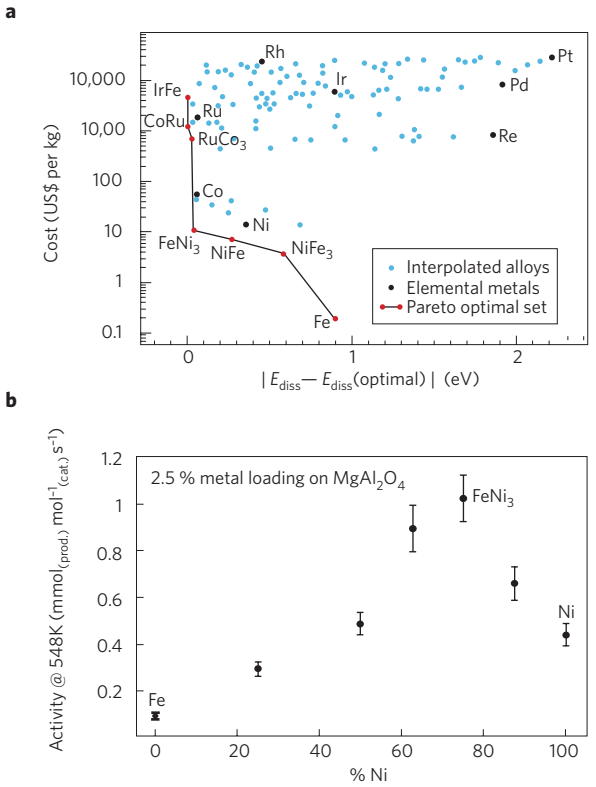

Figure 5 | Computational screening for methanation catalysts. a, A price versus catalytic-performance plot for methanation over a range of elemental metals and alloys. The closer the descriptor E_{diss} (the CO dissociation energy) is to the optimum value (the smaller the value of $|E_{diss}$-E_{diss}(optimal)| is) the better the predicted catalytic activity. The Pareto optimal set of solutions is connected by the solid line, which defines the best compromise between price and catalytic performance for the set of systems investigated theoretically. **b**, Experimental confirmation that NiFe alloys are more active than pure nickel. The error bars indicate the estimated standard deviation of the measured rate of 10%. Adapted from ref. 50; © 2006 Elsevier.

Fig. 6a). Both hydrogenases and nitrogenases have catalytic sites containing sulfur atoms bridged between metal atoms. In looking for inorganic analogues to the active centre in the enzymes it was noted that the same arrangement for sulfur is found at the edge of MoS_2 slabs or nanoparticles. These structures are well-known as hydro-desulfurization catalysts used in removing sulfur-containing molecules from oil products[69,70]. The MoS_2 particles supported on carbon and gold have been tested showing that hydrogen evolution is indeed possible on MoS_2 (refs 63, 71; see Fig. 6b).

Addressing selectivity

Often selectivity towards specific products is of key interest. Selective processes do not only offer cleaner chemistry and better environmental protection, but also allow for improving the use of resources thus leading to more economic production[72].

As selectivity is related to favouring specific reaction pathways among several competing pathways, a prerequisite for the theoretical treatment of selectivity is the accurate treatment of the activity of single reaction pathways. This treatment has to be accomplished at least with sufficient accuracy to address relative changes in the energy barriers between competing pathways.

Ethylene oxide synthesis. Ethylene oxide (EO) is an important chemical with an annual global production of the order of 10 million tons[73]. It is primarily used in organic synthesis reactions. All large-scale production of ethylene oxide is today done by direct partial oxidation of ethylene over a silver catalyst[74]. The selectivity of a typical catalytic EO process is 65% to 80% depending on whether the oxidant is air or pure O_2 (ref. 73). The side product is mainly the full combustion product, CO_2. As the primary expense in the process is the ethylene cost, high selectivity towards EO is important in improving cost-efficiency and minimizing CO_2 emissions.

High-resolution electron energy loss spectroscopy (HREELS) experiments and DFT calculations have shown that an oxametallacycle[75] species is a key intermediate in the ethylene oxide formation over Ag(111) (ref. 76). This has enabled the construction of a detailed DFT-based kinetic model that agrees well with ethylene oxidation rate experiments over Ag (ref. 77). Two competitive transition states lead to ethylene oxide and acetaldehyde, respectively, see Fig. 7a,b. The acetaldehyde eventually goes to full combustion, whereas EO directly desorbs and is unlikely to react further. The difference in energy between these two transition states thus becomes a good descriptor for the selectivity of an EO catalyst, and catalysts, which favour the transition state going towards EO, can be sought computationally[78]. In Fig. 7c the difference in the two transition state energies relative to the difference over silver is shown for a few bimetallic Ag catalysts. It is observed that some presence of copper atoms in the silver surface should yield particularly high selectivity towards EO. The calculations were subsequently verified through the synthesis and testing of a number of Cu/Ag-containing surface alloys. The results are shown in Fig. 7d. It is observed that as the bulk contents of copper increases slightly, the selectivity increases by almost 50% compared with a pure silver reference catalyst[78].

Preferential oxidation of CO in hydrogen. Preferential oxidation of CO in hydrogen (PROX) currently attracts significant attention as an alternative to methanation for removing CO from hydrogen, in particular for fuel-cell applications. The PROX reaction is carried out in a large excess of hydrogen, and the reaction can for example be written as:

$$CO + \tfrac{1}{2}O_2 + H_2 \rightarrow CO_2 + H_2$$

specifying that hydrogen is not consumed in the process. It is very difficult in practice to avoid some hydrogen being oxidized into water. A highly selective catalyst is thus desirable to reduce the amount of CO to an adequate level without combusting too much of the valuable hydrogen. This is of particular importance for hydrogen-consuming applications such as hydrogen proton exchange membrane fuel cells, where even a few tens of ppm CO will poison currently used Pt-based electrocatalysts[79].

On the basis of DFT studies, core–shell nanoparticles have been proposed as candidates for new catalytic properties different from pure metal surfaces, surface alloys and near-surface alloys[80]. Detailed computational studies of platinum-covered ruthenium, iridium, rhodium, palladium, gold and platinum were carried out. These studies suggested that Pt-covered ruthenium, so-called Ru@Pt, could present unique features compared with the other core–shell structures and the pure platinum nanoparticles, as the binding of CO molecules were significantly weakened on the Ru@Pt. The effect of the ruthenium underneath the platinum surface on the CO adsorption is the same electronic effect discussed in connection with Fig. 4: the platinum *d*-states are shifted up in energy due to the ruthenium atoms, and this ligand effect[81] changes the CO bond strength. Experiments have shown that the reaction temperature is significantly lower for PROX over Ru@Pt particles than PtRu alloy, as predicted from calculations. Experiments also show that 70% of the CO is already oxidized to CO_2 at 30°C over the Ru@Pt (ref. 80).

Selective hydrogenation of acetylene. Large-scale production of ethylene is primarily carried out by steam-cracking of saturated hydrocarbons[73], which leads to impurities in the form of acetylene in

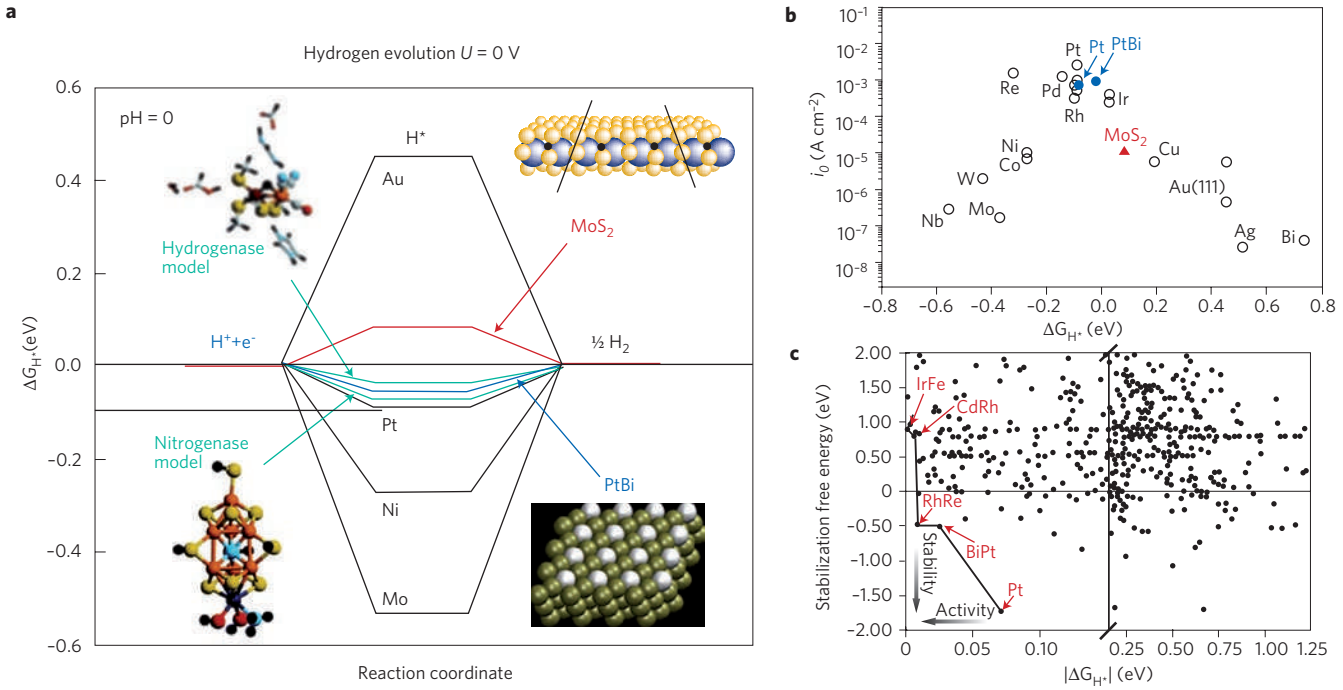

Figure 6 | Screening for hydrogen-evolution catalysts. a, The free energy diagram of hydrogen evolution at zero potential and zero pH for gold, platinum, nickel, molybdenum and PtBi close-packed surfaces, the MoS_2 edge, and the active centres in hydrogenase and nitrogenase. The closer the binding free energy of the intermediate — where H atoms are bound to the catalyst — is to zero the higher the activity. Adapted from ref. 63; © 2005 ACS. **b**, The experimental exchange current, i_0, is plotted as a function of the calculated standard free energy of adsorption of hydrogen, ΔG_{H^*}. Experimental data from many different experiments are included, which accounts for the scatter. In one particular set of experiments (marked in blue) platinum and a PtBi surface alloy are compared. Adapted from ref. 71; © 2007 AAAS. **c**, The stability of different surface alloys is plotted as a function of the binding free energy of hydrogen. In the lower left quadrant are the stable and active surface alloys and the points that limit the set from lower left is the Pareto optimal set. Adapted from ref. 64; © 2006 NPG.

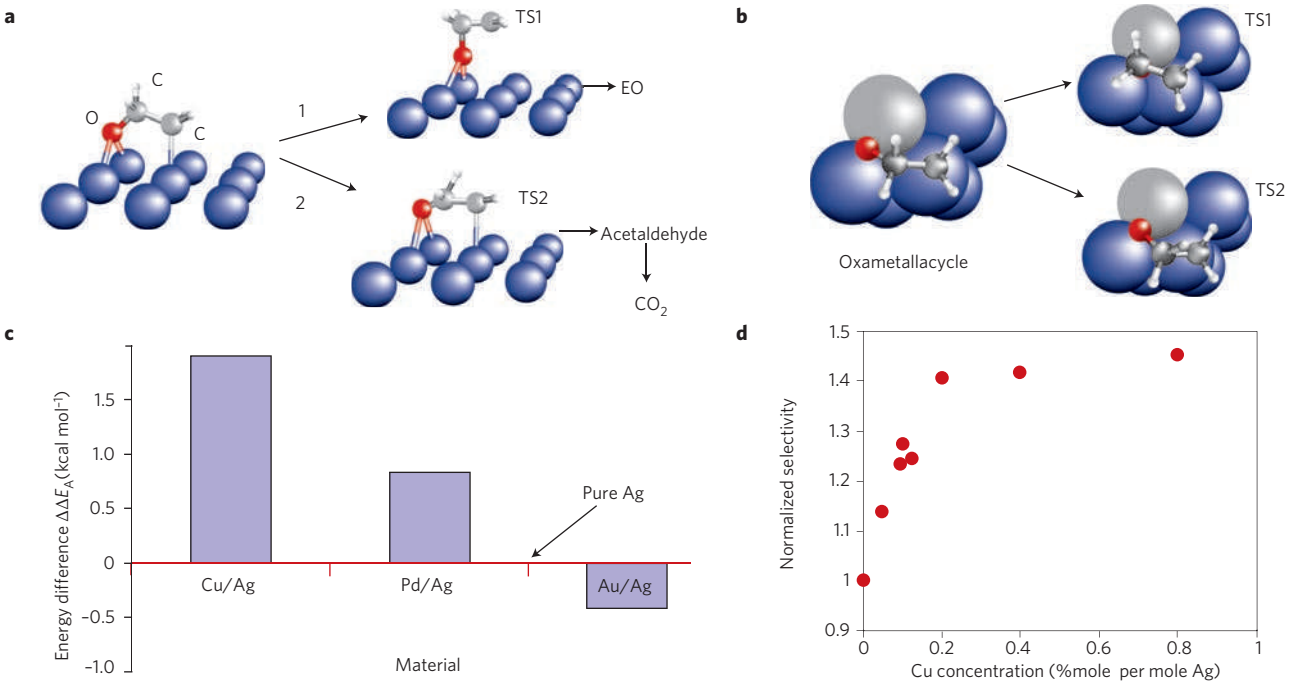

Figure 7 | Computational design of ethylene oxide (EO) synthesis catalysts with improved selectivity. a, Competing oxametallacycle pathways. Activation barriers for the two pathways are calculated to be similar over silver. **b**, Structure of a bimetallic model catalysts. TS is transition state. **c**, The selectivity descriptor, $\Delta\Delta E_A = (\Delta E_{TS2}(\text{alloy}) - \Delta E_{TS1}(\text{alloy})) - (\Delta E_{TS2}(\text{Ag}) - \Delta E_{TS1}(\text{Ag}))$, shown for a number of catalyst compositions. Higher descriptor values means that the bimetallic should be more selective than pure silver. **d**, The measured selectivity relative to pure silver as a function of bulk copper content. All parts adapted from ref. 78; © 2004 Elsevier.

the ethylene product slate. Much of the ethylene is used in processes where acetylene is undesirable. One process where the acetylene is particularly undesired is the important polymerization of ethylene into polyethylene. The acetylene concentration in the ethylene feed can be reduced by selective hydrogenation to ethylene. A high selectivity is necessary to get the acetylene reduced to the desired low levels of a few ppm without hydrogenating ethylene to ethane. The most commonly used catalyst in industry is a silver-modified palladium catalyst.

Density functional theory calculations for a number of transition-metal surfaces show that acetylene and ethylene adsorption energies scale with methyl adsorption energies[82] (Fig. 8a). The slope of the scaling relations in the reactive surface regime is four for C_2H_2 and two for C_2H_4. This can be viewed as a manifestation of bond-order conservation for the surface-bonded carbon atoms[35]. The scaling relations are thus related to bond-order conservation models[83]. A good acetylene hydrogenation catalyst should present a high stability of adsorbed acetylene and a low stability of ethylene. Strong acetylene binding leads to high acetylene removal rate, whereas weak ethylene adsorption leads to ethylene being desorbed instead of further hydrogenation, and therefore high selectivity. This, together with the scaling relations, leads to a window of simultaneously active and selective catalysts as expressed by using the methyl binding energy as a descriptor (see Fig. 8a).

Screening of approximately 70 different alloy surfaces for their methyl binding energies yielded the results shown in Fig. 8b where the constituent cost is plotted versus methyl adsorption energy. A number of alloys fall in the window of interest, including several PdAg alloys, as expected. Also identified are the alloys made from PdGa, PdPb and PdAu, which have recently been shown experimentally to exhibit a good activity and selectivity[84–87]. The alloys CoGa, NiGa, FeZn and NiZn stand out as particularly interesting, because they seem to be active, selective and inexpensive. An analysis of the stability of the different alloys shows that the NiZn alloys are particularly stable, and the NiZn compounds were therefore chosen for further study. In Fig. 8c, the adsorption structures of acetylene and ethylene on the Ni–Zn alloy are shown. The adsorbates are bonded to the nickel sites, which show that the change in adsorption properties is not a result of bonding to the zinc. Instead, the zinc atoms change the electronic properties of the nickel atoms.

A series of NiZn alloy catalysts on $MgAl_2O_4$ spinel supports were synthesized and tested for their selectivity in the hydrogenation of acetylene in a gas mixture of ethylene, acetylene and hydrogen. The ethane production as a function of acetylene conversion is shown

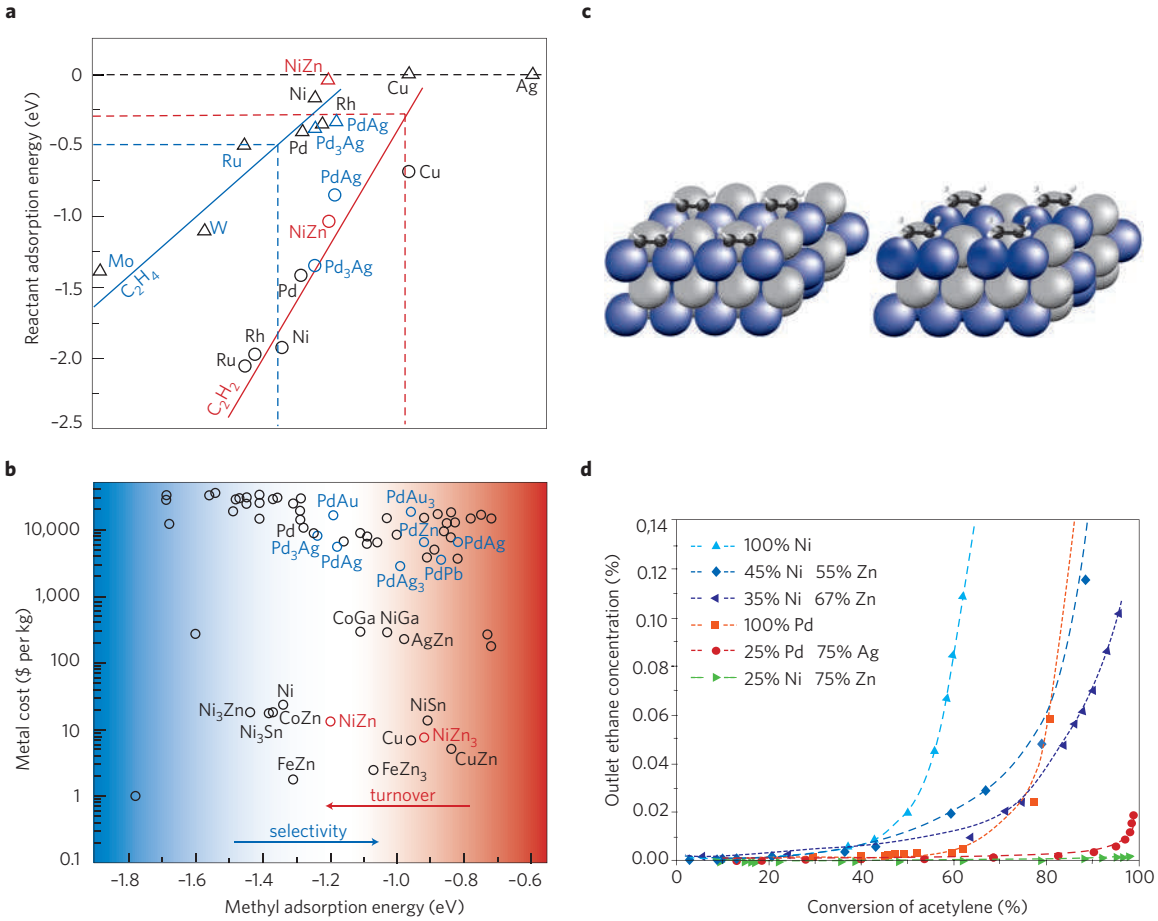

Figure 8 | Identifying catalysts for selective acetylene hydrogenation. a, The calculated binding of acetylene (C_2H_2) and ethylene (C_2H_4) as a function of methyl (CH_3) adsorption over a number of metals and alloys. The solid lines for acetylene (red) and ethylene (blue) identify linear scaling relations. The dotted blue line defines the maximal methyl binding for which the ethylene is predicted to desorb more easily than hydrogenating to ethane. The dotted red line identifies the minimal methyl binding necessary to obtain a turnover frequency on the order of 1 s^{-1}. Together the lines define a window of methyl binding in which catalysts that are simultaneously active and selective are predicted to lie. **b**, Constituent cost of 70 binary intermetallic compounds as a function of their calculated methyl adsorption energies. **c**, The adsorption of acetylene (left) and ethylene (right) on a (bcc-B_2 (110)) structural model of the NiZn catalyst (nickel atoms: blue; zinc atoms: grey). **d**, The measured concentration of ethane at the reactor outlet as a function of acetylene conversion for seven different catalysts. Zero ethane at high conversion is desirable. The experiments verify the theoretical prediction that NiZn catalysts could exhibit selectivity comparable to that of PdAg. All parts adapted from ref. 82; © 2008 AAAS.

in Fig. 8d. A highly selective catalyst will have very low ethane production, even at high conversion, where the amount of acetylene in the reactants is small. Different NiZn catalysts were compared with a model PdAg catalyst. Pure Pd has a reasonably good selectivity, but the PdAg alloy shows a very high selectivity even at high conversions. Nickel is considerably worse than palladium, but as expected from Fig. 8b, adding increasing amounts of zinc increases the selectivity substantially. The NiZn catalyst with the highest zinc content had selectivity comparable to the best PdAg catalyst that was tested.

Outlook

The fact that it has been possible to tailor surfaces with improved catalytic properties from theoretical insights and DFT calculations provides some hope that this may develop into a more generally versatile design strategy. There are, however, a number of challenges ahead.

First, it should be realized that finding leads for new catalysts is only one step towards a new technical catalyst. High catalytic activity or selectivity and low constituent cost can be necessary requirements for a new catalyst, but long-term stability, lack of side-products, resistance to poisons, susceptibility to promoters and cost of production are equally important factors. To some extent these factors may also be simulated, but in the end, experimental studies under realistic conditions will always be central to creating technical catalysts.

An important extension of the notion of DFT-based catalyst design is the use of DFT calculations in reactor design. The first steps in this direction were taken for the ammonia synthesis process in which it proved possible to link the atomic-scale insight obtained by DFT calculations directly with the industrial chemical engineering practice as illustrated in Fig. 9. In an industrial ammonia synthesis reactor there are several catalyst beds with cooling stages in between as illustrated in Fig. 9a. The cooling stages are introduced so as to operate as close to the maximum rate line (red in Fig. 9a) as possible. The important notion is that the position of the maximum for the volcano curve (Fig. 9b) is a strong function of the operating conditions. At low ammonia concentrations (reactor inlet), Fe is the preferred elemental catalyst, whereas at high ammonia concentrations (reactor outlet), Ru is the preferred elemental catalyst. The optimal catalyst curves (Fig. 9c) express the properties of the optimal catalyst at given reaction conditions plotted with the operating line. Thus, this illustrates the value(s) of the activity descriptor(s) at the maximum of the volcano curve at the given reaction conditions. The key concept is that the structure and composition of the optimal catalyst is a function of the reaction conditions, and as these vary throughout industrial reactors, it is desirable to perform the computational screening as a function of all possible reaction conditions. This might also, in a longer perspective, be a way to identify radically new catalysts rather than simply improving the performance of known catalysts.

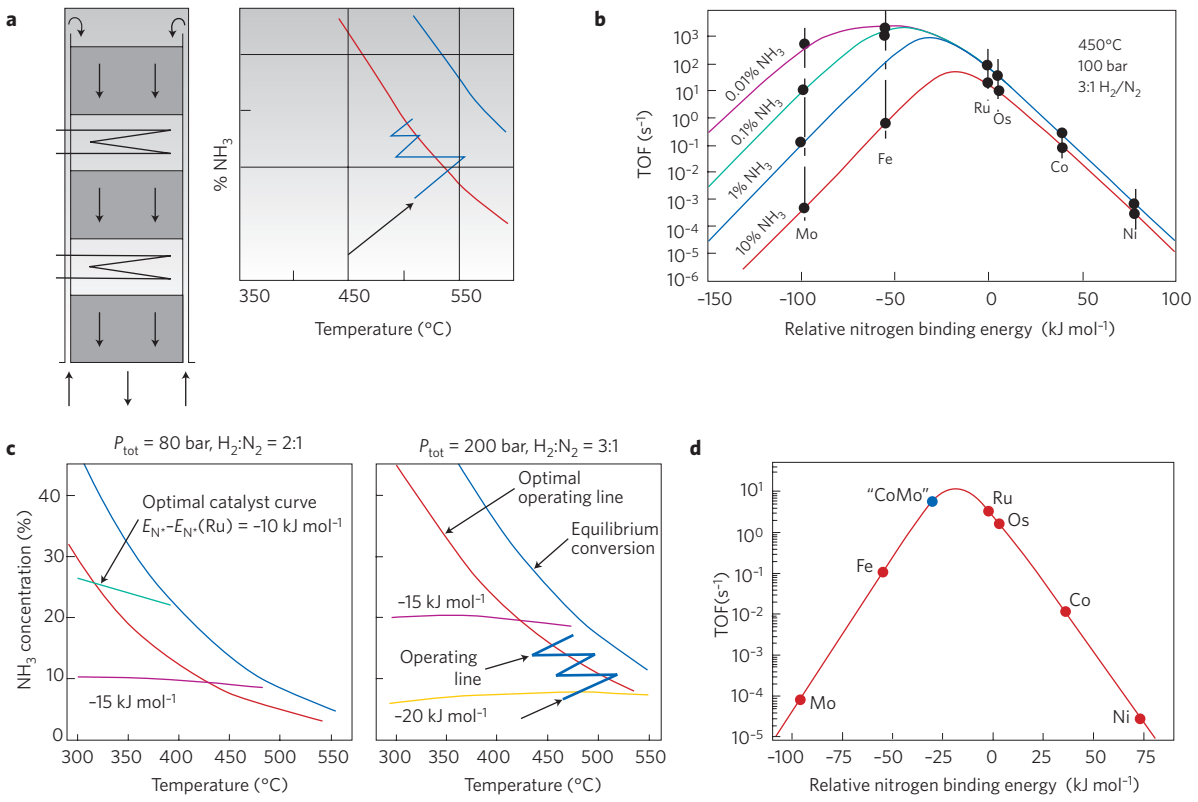

Figure 9 | Linking DFT calculations with industrial reactor design and catalyst selection. a, Schematic illustration of an industrial ammonia synthesis reactor with three adiabatic catalyst beds and two cooling stages. The diagram shows the equilibrium line, the optimal operating line, which can also be called maximum rate line (red), and the operating line for the reactor configuration shown. The closer the operating line approaches the optimal operating line, the lower the catalyst volume required. **b**, Volcano curves for the turnover frequency, TOF, calculated based on micro-kinetic modelling using parameters calculated by DFT. **c**, An optimal catalyst curve expresses the reaction conditions under which a transition metal surface with a given nitrogen binding energy is the theoretically optimal catalyst. The optimal catalyst curves make it possible to identify desirable catalysts for relevant reaction conditions. E_{N^*} is the metal–nitrogen binding energy (negative values signify exothermic adsorption). **d**, The interpolation concept illustrating that the binding energy for a CoMo catalyst is intermediate between that of the elemental catalysts Co and Mo (ref. 46). With this concept, or other alloy models, it is possible to identify suitable catalyst leads to be used with the optimal catalyst curves, that is, to design catalysts for specific rector design and process conditions. Figure adapted from ref. 100; © 2002 Elsevier.

The examples discussed in this review all refer to catalysts where the active site consists of a transition metal (alloy) surface. It is implicitly assumed that the surface of the supported nanoparticles can be modelled by extended surfaces, perhaps with defects. Much more work is required to find out when this assumption breaks down and how one then systematically includes support effects directly in the simulations. Going beyond transition metal catalysts may also provide a considerable challenge from a theoretical point of view. From detailed comparisons between theory and experiment we know that DFT works quite well for these systems, but we also know that it may work less well for other classes of catalysts including for example some strongly correlated oxides[88–91]. There are also a number of situations where it is essential to include van der Waals interactions[92]. Recent developments suggest that this may become a possibility in the near future[93,94]. Additional challenges are related to finding methods to determine the ground-state structures of unknown materials[95–97]. We also need to describe the interaction of more complicated molecules with all these possible surface structures, and additional complications arise in describing electrocatalytic and photocatalytic processes.

Although experimental methods usually tend to become more expensive with time, computational methods will become cheaper as computers become faster. In combination with new developments in electronic structure theory and computational methods, this suggests that computational approaches for the discovery and development of catalysts hold great promise for the future.

Acknowledgements

The Center for Atomic-scale Materials Design is funded by the Lundbeck Foundation. J.K.N. acknowledges support from Ib Henriksens Fond.

Additional information

The authors declare competing financial interests: details accompany the full-text HTML version of the paper at www.nature.com/naturechemistry. Correspondence should be addressed to J.K.N.

References

1. Thomas, J. M. & Thomas, W.-J. *Principle and Practice of Heterogeneous Catalysis* (VCH, 1997).
2. Ceder, G. *et al.* Identification of cathode materials for lithium batteries guided by first-principles calculations. *Nature* **392,** 694–696 (1998).
3. Alapati, S. V., Johnson, J. K. & Sholl, D. S. Using first principles calculations to identify new destabilized metal hydride reactions for reversible hydrogen storage. *Phys. Chem. Chem. Phys.* **9,** 1438–1452 (2007).
4. Piquini, P., Graf, P. A. & Zunger, A. Band-gap design of quaternary (In, Ga)(As, Sb) semiconductors via the inverse-band-structure approach. *Phys. Rev. Lett.* **100,** 186403 (2008).
5. Wondimagegn, T., Wang, D., Razavi, A. & Ziegler, T. Computational design of C-2-symmetric metallocene-based catalysts for the synthesis of high molecular weight polymers from ethylene/propylene copolymerization. *Organometallics* **27,** 6434–6439 (2008).
6. Conley, B. L. *et al.* Design and study of homogeneous catalysts for the selective, low temperature oxidation of hydrocarbons. *J. Mol. Cat. A-Chem.* **251,** 8–23 (2006).
7. Nilsson, A., Pettersson, L. G. M. & Nørskov, J. K. (eds) *Chemical Bonding at Surfaces and Interfaces* (Elsevier, 2008).
8. Ertl, G. Reactions at surfaces: from atoms to complexity. *Angew. Chem. Int. Ed.* **47,** 3524–3535 (2008).
9. Somorjai, G. A. *Introduction to Surface Chemistry and Catalysis* (Wiley, 1994).
10. Yeo, Y. Y., Vattuone, L. & King, D. A. Calorimetric heats for CO and oxygen adsorption and for the catalytic CO oxidation reaction on Pt{111}. *J. Chem. Phys.* **106,** 392–401 (1997).
11. Goodman, D. W., Kelley, R. D., Madey, T. E. & Yates, J. T. Kinetics of the hydrogenation of CO over a single crystal nickel-catalyst. *J. Catal.* **63,** 226–234 (1980).
12. Lytken, O. *et al.* Energetics of cyclohexene adsorption and reaction on Pt(111) by low-temperature microcalorimetry. *J. Am. Chem. Soc.* **130,** 10247–10257 (2008).
13. Kohn, W. & Sham, L. J. Self-consistent equations including exchange and correlation effects. *Phys. Rev. A* **140**, 1133–1138 (1965).
14. Perdew, J. P., Burke, K. & Ernzerhof, M. Generalized gradient approximation made simple. *Phys. Rev. Lett.* **77,** 3865–3868 (1996).
15. Hammer, B., Hansen, L. B. & Nørskov, J. K. Improved adsorption energetics within density functional theory using revised PBE functionals. *Phys. Rev. B* **59,** 7413–7421 (1999).
16. Hammer, B. & Nørskov, J. K. Theoretical surface science and catalysis — calculations and concepts. *Adv. Catal.* **45,** 71–129 (2000).
17. Hansen, E. W. & Neurock, M. First-principles-based Monte Carlo simulation of ethylene hydrogenation kinetics on Pd. *J. Catal.* **196,** 241–252 (2000).
18. Reuter, K., Frenkel, D. & Scheffler, M. The steady state of heterogeneous catalysis, studied by first-principles statistical mechanics. *Phys. Rev. Lett.* **93,** 116105 (2004).
19. Honkala, K. *et al.* Ammonia synthesis from first-principles calculations. *Science* **307,** 555–558 (2005).
20. Kandoi, S. *et al.* Prediction of experimental methanol decomposition rates on platinum from first principles. *Top. Catal.* **37,** 17–28 (2006).
21. Hansen, K. H. *et al.* Palladium nanocrystals on Al_2O_3: Structure and adhesion energy. *Phys. Rev. Lett.* **83,** 4120–4123 (1999).
22. Hansen, T. W. *et al.* Atomic-resolution *in situ* transmission electron microscopy of a promoter of a heterogeneous catalyst. *Science* **294,** 1508–1510 (2001).
23. Hansen, P. L. *et al.* Atom-resolved imaging of dynamic shape changes in supported copper nanocrystals. *Science* **295,** 2053–2055 (2002).
24. Hofmann, S. *et al. In situ* observations of catalyst dynamics during surface-bound carbon nanotube nucleation. *Nano Lett.* **7,** 602–608 (2007).
25. Gontard, L. C. *et al.* Aberration-corrected imaging of active sites on industrial catalyst nanoparticles. *Angew. Chem. Int. Ed.* **46,** 3683–3685 (2007).
26. Kohn, W. Density functional and density matrix method scaling linearly with the number of atoms. *Phys. Rev. Lett.* **76,** 3168–3171 (1996).
27. Prodan, E. & Kohn, W. Nearsightedness of electronic matter. *Proc. Natl Acad. Sci. USA* **102,** 11635–11638 (2005).
28. Nørskov, J. K. *et al.* Universality in heterogeneous catalysis. *J. Catal.* **209,** 275–278 (2002).
29. Ciobica, I. M. & van Santen, R. A. Carbon monoxide dissociation on planar and stepped Ru(0001) surfaces. *J. Phys. Chem. B* **107,** 3808–3812 (2003).
30. Pallassana, V. & Neurock, M. Electronic factors governing ethylene hydrogenation and dehydrogenation activity of pseudomorphic Pd-ML/Re(0001), Pd-ML/Ru(0001), Pd(111), and Pd-ML/Au(111) surfaces. *J. Catal.* **191,** 301–317 (2000).
31. Alcalá, R., Mavrikakis, M. & Dumesic, J. A. DFT studies for cleavage of C-C and C-O bonds in surface species derived from ethanol on Pt(111). *J. Catal.* **218,** 178–190 (2003).
32. Michaelides, A. *et al.* Identification of general linear relationships between activation energies and enthalpy changes for dissociation reactions at surfaces. *J. Am. Chem. Soc.* **125,** 3704–3705 (2003).
33. Bligaard, T. *et al.* The Brønsted-Evans-Polanyi relation and the volcano curve in heterogeneous catalysis. *J. Catal.* **224,** 206–217 (2004).
34. Sabatier, P. Hydrogénations et déshydrogénations par catalyse. *Ber. Deutsch. Chem. Gesellshaft* **44,** 1984–2001 (1911).
35. Abild-Pedersen, F. *et al.* Scaling properties of adsorption energies for hydrogen-containing molecules on transition-metal surfaces. *Phys. Rev. Lett.* **99,** 016105 (2007).
36. Boudart, M. in *Handbook of Heterogeneous Catalysis* (eds Ertl, G., Knözinger, H. & Weitkamp, J.) 1 (Wiley-VCH, Weinheim, 1997).
37. Falsig, H. *et al.* Trends in the catalytic CO oxidation activity of nanoparticles. *Angew. Chem. Int. Ed.* **47,** 4835–4835 (2008).
38. Cheng, J. & Hu, P. Utilization of the three-dimensional volcano surface to understand the chemistry of multiphase systems in heterogeneous catalysis. *J. Am. Chem. Soc.* **130,** 10868–10869 (2008).
39. Holloway, S., Lundqvist, B. I. & Nørskov, J. K. in *Proc. 8th Conference on Catalysis, Berlin* vol. IV, p.85 (Verlag Chemie, 1984).
40. Hammer, B. & Nørskov, J. K. Why gold is the noblest of all the metals. *Nature* **376,** 238–240 (1995).
41. Mavrikakis, M., Hammer, B. & Nørskov, J. K. Effect of strain on the reactivity of metal surfaces. *Phys. Rev. Lett.* **81,** 2819–2822 (1998).
42. Roudgar, A. & Gross, A. Local reactivity of metal overlayers: Density functional theory calculations of Pd on Au. *Phys. Rev. B* **67,** 33409 (2003).
43. Gajdos, M., Eichler, A. & Hafner, J. CO adsorption on close-packed transition and noble metal surfaces: trends from ab initio calculations. *J. Phys. Condens. Matter* **16,** 1141–1164 (2004).
44. Nilsson, A. *et al.* The electronic structure effect in heterogeneous catalysis. *Catal. Lett.* **100** 111–114 (2005).
45. Besenbacher, F. *et al.* Design of a surface alloy catalyst for steam reforming. *Science* **279,** 1913–1915 (1998).
46. Jacobsen, C. J. H. *et al.* Catalyst design by interpolation in the periodic table: Bimetallic ammonia synthesis catalysts. *J. Am. Chem. Soc.* **123,** 8404–8405 (2001).

47. Toulhoat, H. & Raybaud, P. Kinetic interpretation of catalytic activity patterns based on theoretical chemical descriptors. *J. Catal.* **216,** 63–72 (2003).
48. Strasser, P. *et al.* High throughput experimental and theoretical predictive screening of materials. A comparative study of search strategies for new fuel cell anode catalysts. *Phys. Chem. B* **107,** 11013–11021 (2003).
49. Greely, J. & Mavrikakis, M. Alloy catalysts designed from first principles. *Nature Mater.* **3,** 810–815 (2004).
50. Andersson, M. P. *et al.* Toward computational screening in heterogeneous catalysis: Pareto-optimal methanation catalysts. *J. Catal.* **239,** 501–506 (2006).
51. Sabatier, P. & Senderens, J. B. New methane synthesis. *Compte Rendu Acad. Sci. Paris* **134,** 514–516 (1902).
52. Sehested, J. *et al.* Discovery of technical methanation catalysts based on computational screening. *Top. Catal.* **45,** 9–13 (2007).
53. Jinnouchi, R. & Anderson, A. B. Aqueous and surface redox potentials from self-consistently determined Gibbs energies. *J. Phys. Chem. C* **112,** 8747–8750 (2008).
54. Rossmeisl, J., Skúlason, E., Björketun, M. E., Tripkovic, V. & Nørskov, J. K. Modeling the electrified solid-liquid interface. *Chem. Phys. Lett.* **466,** 68–71 (2008).
55. Shubina, T. E. & Koper, M. T. M. Co-adsorption of water and hydroxyl on a Pt_2Ru surface. *Electrochem. Commun.* **8,** 703–706 (2006).
56. Roudgar, A. & Gross, A. Water bilayer on the Pd/Au(111) overlayer system: Coadsorption and electric field effects. *Chem. Phys. Lett.* **409,** 157–162 (2005).
57. Sugino, O. *et al.* First-principles molecular dynamics simulation of biased electrode/solution interface. *Surf. Sci.* **601,** 5237–5240 (2007).
58. Filhol, J. S. & Neurock, M. Elucidation of the electrochemical activation of water over Pd by first principles. *Angew. Chem. Int. Ed.* **45,** 402–406 (2006).
59. Conway, B. E. & Bockris, J. O. M. Electrolytic hydrogen evolution kinetics and its relation to the electronic and adsorptive properties of the metal. *J. Chem. Phys.* **26,** 532–541 (1957).
60. Parsons, R. The rate of electrolytic hydrogen evolution and the heat of adsorption of hydrogen. *Trans. Faraday Soc.* **54,** 1053–1063 (1958).
61. Trasatti, S. Work function, electronegativity, and electrochemical behavior of metals.3. Electrolytic hydrogen evolution in acid solutions. *J. Electroanal. Chem.* **39,** 163–184 (1972).
62. Nørskov, J. K. *et al.* Trends in the exchange current for hydrogen evolution. *J. Electrochem. Soc.* **152** J23-J26 (2005).
63. Hinnemann, B. *et al.* Biomimetic hydrogen evolution. *J. Am. Chem. Soc.* **127,** 5308–5309 (2005).
64. Greeley, J. *et al.* Computational high-throughput screening of electrocatalytic materials for hydrogen evolution. *Nature Mater.* **5,** 909–913 (2006).
65. Gómez, R., Feliu, J. M. & Aldaz, A. Effects of irreversibly adsorbed bismuth on hydrogen adsorption and evolution on Pt(111). *Electrochim. Acta* **42,** 1675–1683 (1997).
66. Evans, D. J. & Pickett, C. J. Chemistry and the hydrogenases. *Chem. Soc. Rev.* **32,** 268–275 (2003).
67. Rees, D. C. & Howard, J. B. The interface between the biological and inorganic worlds: Iron-sulfur metalloclusters. *Science* **300,** 929–931 (2003).
68. Siegbahn, P. E. M., Tye, J. W. & Hall, M. B. Computational studies of [NiFe] and [FeFe] hydrogenases. *Chem Rev.* **107,** 4414–4435 (2007).
69. Topsøe, H., Clausen, B. S. & Massoth, F. E. in *Catalysis, Science and Technology* Vol. 11 (eds Anderson, J. R. & Boudart, M.) 1–310 (Springer, 1996).
70. Helveg, S. *et al.* Atomic-scale structure of single-layer MoS_2 nano-clusters. *Phys. Rev. Lett.* **84,** 951–954 (2000).
71. Jaramillo, T. F. *et al.* Identification of active edge sites for electrochemical H_2 evolution from MoS_2 nanocatalysts. *Science* **317,** 100–102 (2007).
72. Somorjai, G. A. & Yang, M. The surface science of catalytic selectivity. *Top. Catal.* **24,** 61–72 (2003).
73. Weissermel, K. & Arpe, H.-J. *Industrial Organic Chemistry.* 4th edn (Wiley-VCH, 2003).
74. Lefort, T. E. Process for the production of ethylene oxide. French Patent 729952 (1931).
75. Brainard, R. L. & Madix, R. J. Surface-mediated isomerization and oxidation of allyl alcohol on Cu(110). *J. Am. Chem. Soc.* **111,** 3826–3835 (1989).
76. Linic, S. & Barteau, M. A. Formation of a stable surface oxametallacycles that produces ethylene oxide. *J. Am. Chem. Soc.* **124,** 310–317 (2002).
77. Linic, S. & Barteau, M. A. Construction of a reaction coordinate and a microkinetic model for ethylene epoxidation on silver from DFT calculations and surface science experiments. *J. Catal.* **214,** 200–212 (2003).
78. Linic, S., Jankowiak, J. & Barteau, M. A. Selectivity driven design of bimetallic ethylene epoxidation catalysts from first principles. *J. Catal.* **224,** 489–493 (2004).
79. Lemons, R. A. Fuel-cells for transportation. *J. Power Sources* **29,** 251–264 (1990).
80. Alayoglu, S., Nilekar, A. U., Mavrikakis, M. & Eichhorn, B. Ru-Pt core-shell nanoparticles for preferential oxidation of carbon monoxide in hydrogen. *Nature Mater.* **7,** 333–338 (2008).
81. Liu, P., Logadottir, A. & Nørskov, J. K. Modeling the electro-oxidation of CO and H_2/CO on Pt, Ru, PtRu and Pt_3Sn. *Electrochim. Acta* **48,** 3731–3742 (2003).
82. Studt, F. *et al.* Identification of non-precious metal alloy catalysts for selective hydrogenation of acetylene. *Science* **320,** 1320–1322 (2008).
83. Shustorovich, E. & Bell, A. T. The thermochemistry of C-2 hydrocarbons on transition-metal surfaces - the bond-order-conservation approach. *Surf. Sci.* **205,** 492–512 (1988).
84. Kovnir, K. *et al.* A new approach to well-defined, stable and site-isolated catalysts. *Sci. Technol. Adv. Mater.* **8,** 420–427 (2007).
85. Volpe, M. A., Rodriguez, P. & Gigola, C. E. Preparation of Pd-Pb/α-Al_2O_3 catalysts for selective hydrogenation using $PbBu_4$: the role of metal-support boundary atoms and the formation of a stable surface complex. *Catal. Lett.* **61,** 27–32 (1999).
86. Choudhary, T. V., Sivadinarayana, C., Datye, A. K., Kumar, D. & Goodman, D. W. Acetylene hydrogenation on Au-based catalysts. *Catal. Lett.* **86,** 1–8 (2003).
87. Blankenship, S. A., Voight, R. W., Perkins, J. A. & Fried, J. E. Process for selective hydrogenation of acetylene in an ethylene purification process. US Patent 6,509,292 (2003).
88. Kohan, A. F., Ceder, G., Morgan, D. & van de Walle, C. G. First-principles study of native point defects in ZnO. *Phys. Rev. B* **61,** 15019–15027 (2000).
89. Solans-Monfort, X., Branchadell, V., Sodupe, M., Sierka, M. & Sauer, J. Electron hole formation in acidic zeolite catalysts. *J. Chem. Phys.* **121,** 6034–6041 (2004).
90. Pacchioni, G. Modeling doped and defective oxides in catalysis with density functional theory methods: Room for improvements. *J. Chem. Phys.* **128,** 182505 (2008).
91. Chretien, S. & Metiu, H. O_2 evolution on a clean partially reduced rutile TiO_2(110) surface and on the same surface precovered with Au_1 and Au_2: The importance of spin conservation. *J. Chem. Phys.* **129,** 074705 (2008).
92. Eder, F. & Lercher, J. A. Alkane sorption in molecular sieves: The contribution of ordering, intermolecular interactions, and sorption on Brønsted acid sites. *Zeolites* **18,** 75–81 (1997).
93. Dion, M., Rydberg, H., Schroder, E., Langreth, D. C. & Lundqvist, B. I. Van der Waals density functional for general geometries. *Phys. Rev. Lett.* **92,** 246401 (2004).
94. Chakarova-Kack, S. D., Schroder, E., Lundqvist, B. I. & Langreth, D. C. Application of van der Waals density functional to an extended system: Adsorption of benzene and naphthalene on graphite. *Phys. Rev. Lett.* **96,** 146107 (2006).
95. Johannesson, G. H. *et al.* Combined electronic structure theory and evolutionary search for materials design. *Phys. Rev. Lett.* **88,** 255506 (2002).
96. Curtarolo, S., Morgan, D., Persson, K., Rodgers, J. & Ceder, G. Predicting crystal structures with data mining of quantum calculations. *Phys. Rev. Lett.* **91,** 135503 (2003).
97. Oganov, A. R. & Glass, C. W. Crystal structure prediction using ab initio evolutionary techniques: Principles and applications. *J. Chem. Phys.* **124,** 244704 (2006).
98. Newns, D. M. Self-consistent model of hydrogen chemisorption. *Phys. Rev.* **178,** 1123–1135 (1969).
99. Kitchin, J. R., Nørskov, J. K., Barteau, M. A. & Chen, J. G. Modification of the surface electronic and chemical properties of Pt(111) by subsurface 3d transition metals. *J. Chem. Phys.* **120,** 10240–10245 (2004).
100. Jacobsen, C. J. H., Dahl, S., Boisen, A., Clausen, B. S. & Nørskov, J. K. Optimal catalyst curves: Connecting DFT calculations with industrial reactor design and catalyst selection. *J. Catal.* **205,** 382–387 (2002).